

Controlled Gaussian Process Dynamical Models with Application to Robotic Cloth Manipulation

Fabio Amadio¹, Juan Antonio Delgado-Guerrero², Adrià Colomé², and Carme Torras²

Abstract—Over the last years, robotic cloth manipulation has gained relevance within the research community. While significant advances have been made in robotic manipulation of rigid objects, the manipulation of non-rigid objects such as cloth garments is still a challenging problem. The uncertainty on how cloth behaves often requires the use of model-based approaches. However, cloth models have a very high dimensionality. Therefore, it is difficult to find a middle point between providing a manipulator with a dynamics model of cloth and working with a state space of tractable dimensionality. For this reason, most cloth manipulation approaches in literature perform static or quasi-static manipulation. In this paper, we propose a variation of Gaussian Process Dynamical Models (GPDMs) to model cloth dynamics in a low-dimensional manifold. GPDMs project a high-dimensional state space into a smaller dimension latent space which is capable of keeping the dynamic properties. Using such approach, we add control variables to the original formulation. In this way, it is possible to take into account the robot commands exerted on the cloth dynamics. We call this new version Controlled Gaussian Process Dynamical Model (C-GPDM). Moreover, we propose an alternative kernel representation for the model, characterized by a richer parameterization than the one employed in the majority of previous GPDM realizations. The modeling capacity of our proposal has been tested in a simulated scenario, where C-GPDM proved to be capable of generalizing over a considerably wide range of movements and correctly predicting the cloth oscillations generated by previously unseen sequences of control actions.

I. INTRODUCTION

Robotic cloth manipulation has a wide range of applications, from textile industry to assistive robotics. However, the complexity of cloth behaviour results in a high uncertainty in the state transition given a certain action. This uncertainty is what makes cloth manipulation much harder than manipulating rigid objects. Intuitively, using a cloth model is the solution to reduce such uncertainty by knowing an approximation of cloth dynamics. In literature, we can find several cloth models that simulate the internal cloth state [1], [2], [3]. They represent cloth as a mesh of material points, and simulate their behaviour taking into account physical constraints. However, such models need not only to behave similarly enough to the cloth garment, but to have a tractable dimension, for computational reasons. Imagine a piece of cloth e.g. a square towel. If we build an 8×8

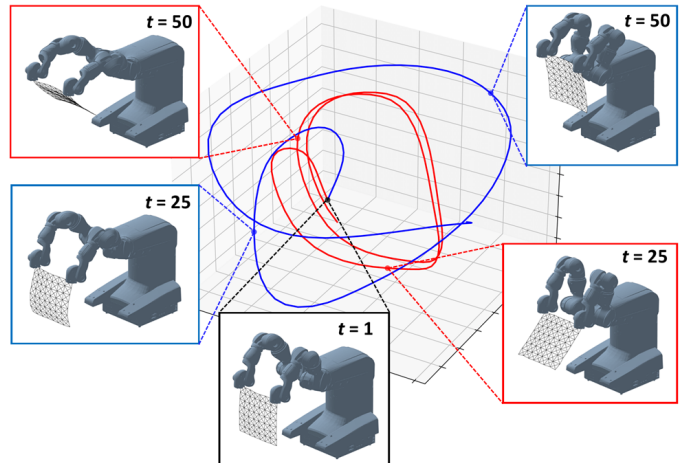


Fig. 1: The same C-GPDM predicts two distinct latent state trajectories in response to two different sequences of unseen control actions. Each point in the latent space has associated a particular configuration of the modeled cloth.

cloth mesh, and characterize the three Cartesian components of each point, the cloth state results in a 192-dimensional manifold. Such dimensionality is unmanageable, not only in terms of computational costs, but also for building a tractable state-action space policy. Such is the case of [4], where simulated results are obtained after hours of computations. Therefore, Dimensionality Reduction (DR) methods become necessary for this approach.

In [5], linear DR techniques were used for learning cloth manipulation by biasing the latent space projection with each execution's performance. Nonlinear methods, such as Gaussian Process Latent Variable Models (GPLVM) [6] have also been applied for this purpose. In [7], GPLVM was employed to project task-specific motor-skills of the robot onto a much smaller state representation, whereas in [8] GPLVM was also used to represent a robot manipulation policy in a latent space, taking contextual features into account. However, these approaches focus the dimensionality reduction in the robot action characterization, rather than in the manipulated object's dynamics. Instead, in [9] the same DR technique was applied to learn a latent representation of the cloth state from point cloud observations taken with a motion capture system and depth sensors. However, such approach did not consider the dynamics of the cloth handling task, and its applicability is limited to a quasi-static manipulation.

To address this issue, we consider Gaussian Process Dynamical Models (GPDM), firstly introduced in [10], which are an

This work was partially developed in the context of the project CLOTHILDE ("CLOTH manipulation Learning from DEMonstrations"), which has received funding from the European Research Council (ERC) under the European Union's Horizon 2020 research and innovation programme (Advanced Grant agreement No 741930). This work is also supported by the Spanish State Research Agency through the María de Maeztu Seal of Excellence to IRI MDM-IP-2018-05.

¹Department of Information Engineering, Università di Padova, Italy amadiofa@dei.unipd.it

²Institut de Robòtica i Informàtica Industrial (IRI), CSIC-UPC, Spain [jdelgado, acolome, torras]@iri.upc.edu

extension of the GPLVM structure explicitly oriented to the analysis of high-dimensional time series. GPDMs have been applied in several different fields, from human motion tracking [11], [12] to dynamic texture modeling [13]. In the context of cloth manipulation, GPDMs were adopted in [14] to learn a latent model of the dynamics of a clothing task. However, this framework, as it is, lacks in its structure a fundamental component to correctly describe the dynamics of a system, namely control actions, limiting the generalization capacity of the model.

Therefore, we propose in this work an extension of the GPDM structure, that takes into account the influence of external control actions on the modeled dynamics. We call it *Controlled Gaussian Process Dynamical Models* (C-GPDMs). In this new version of the model, control actions directly affect the dynamics in the latent space. Thus, a C-GPDM, trained on a sufficiently diverse set of interactions, is able to predict the effects of control actions never experienced before inside a space of reduced dimensions, and then reconstruct high-dimensional motions by projecting the latent state trajectories into the observation space. We tested the applicability of such solution in a simulated cloth manipulation task with a bimanual robot. C-GPDM has proved capable of fitting different types of cloth movement, and predict the results of sequences of control actions never seen during training. As an example, in Fig. 1, we show the trajectories predicted by the same C-GPDM subject to two different sequences of control actions. Note how the two latent trajectories, starting from the same initial state, are driven by their respective control actions into different regions of the latent space, where different cloth poses are reconstructed.

Furthermore, we propose changes to the kernel functions from the ones usually adopted in the context of GPDM. In fact, for this class of models, in many previous works [10], [11], [12], Gaussian processes (GPs) are equipped with RBF and linear kernel functions that are characterized by a small number of tunable parameters. For C-GPDM, we introduced a richer parameterization in both latent and dynamic mappings, obtaining an improvement in the accuracy of predicted trajectories. Also [13] focused on kernel structures for GPDMs, and proposed a multi-kernel structure for the GPs that model the dynamics, but it kept kernel functions unchanged in the latent map.

The remainder of the paper is structured as follows. Preliminaries are given in Sec. II. C-GPDM framework is presented in Sec. III. Sec. IV treats its training and explains how to make predictions, in both latent and observation spaces. Experimental results on a simulated robotic cloth manipulation scenario are reported in Sec. V. Finally, Sec. VI draws the conclusions.

II. PRELIMINARIES: FROM GPs TO GPDMs

Gaussian Processes [15] are the infinite-dimensional generalization of multivariate Gaussian distributions. They are defined as infinite-dimension stochastic processes such that, for any finite set of input locations $\mathbf{x}_1, \dots, \mathbf{x}_n$, the random variables $f(\mathbf{x}_1), \dots, f(\mathbf{x}_n)$ have joint Gaussian distributions. A GP is completely defined by its mean function $m(\mathbf{x})$ and its

covariance function $k(\mathbf{x}, \mathbf{x}')$, often referred to as kernel, that must be symmetric and positive semi-definite. Usually GPs are indicated as

$$f(\mathbf{x}) \sim \mathcal{GP}(m(\mathbf{x}), k(\mathbf{x}, \mathbf{x}')).$$

GPs can be used for regression models of the form $\mathbf{y} = f(\mathbf{x}) + \varepsilon$, with ε an i.i.d. Gaussian noise, as they provide closed formulae to predict new values of the response variable \mathbf{y}^* , given new input location values \mathbf{x}^* .

Based on such formulation, GPLVM [6] and its variations [16] emerged as feature extraction methods that can be used as multiple-output GP regression models. In this way, these models, under a DR perspective, associate and learn low-dimensional representations of higher-dimensional observed data, assuming that observed variables are determined by the latent ones. Finally, GPLVMs provide, as a result of an optimization, a mapping from the latent space to the observation space, together with a set of latent variables representing the observed values. However, GPLVMs are not explicitly thought to deal with data from time series, where observations at different time steps are connected by some form of dynamics.

Thus, [10] firstly introduced Gaussian Process Dynamical Models (GPDM), an extension of the GPLVM structure explicitly oriented to the analysis of high-dimensional time series. A GPDM entails essentially two stages: (i) a latent mapping that projects high-dimensional observations to lower dimensional latent states (1); (ii) a discrete-time Markovian dynamics that captures the evolution of the time series inside the reduced latent space (2). GPs are used to model both the latent map, as in GPLVMs, and the undergoing dynamics transition function. GPDMs are then defined by

$$\mathbf{y}_t = g(\mathbf{x}_t) + \mathbf{n}_{y,t}, \quad (1)$$

$$\mathbf{x}_{t+1} = h(\mathbf{x}_t) + \mathbf{n}_{x,t}, \quad (2)$$

where \mathbf{y}_t is the high-dimensional observation vector and \mathbf{x}_t represents the latent state, at time step t . Here, $\mathbf{n}_{y,t}$ and $\mathbf{n}_{x,t}$ are two zero-mean isotropic white Gaussian noise processes, while g and h indicate the unknown functions characterizing the two maps.

III. CONTROLLED GPDM

Let us consider a system governed by an unknown dynamics. At each time step t , it is possible to influence it by applying control actions $\mathbf{u}_t \in \mathbb{R}^E$ and get an observation $\mathbf{y}_t \in \mathbb{R}^D$. For highly dimensional observation spaces, it could be unfeasible to directly model the evolution of a sequence of observations in response to a series of inputs. In this context, it could be convenient to capture the dynamics of the system in a lower dimensional latent space \mathbb{R}^d , with $d \ll D$. Let $\mathbf{x}_t \in \mathbb{R}^d$ be the latent state associated to \mathbf{y}_t . We propose to use a variation of the GPDM that keeps into account the influence of control actions, while maintaining the dimensionality reduction properties of the original model. We call it *Controlled Gaussian Process Dynamical Model* (C-GPDM).

A C-GPDM consists of a latent map (3) projecting observations \mathbf{y}_t into latent states \mathbf{x}_t , and a dynamics map (4) that

describes the evolution of the latent state \mathbf{x}_t , subject to control action \mathbf{u}_t .

$$\mathbf{y}_t = g(\mathbf{x}_t) + \mathbf{n}_{y,t}, \quad (3)$$

$$\mathbf{x}_{t+1} - \mathbf{x}_t = h(\mathbf{x}_t, \mathbf{u}_t) + \mathbf{n}_{x,t}. \quad (4)$$

Differently from original GPDM (2), control actions have influence on C-GPDM transition function (4). On the other hand, latent map (3) is identical to (1) because control actions should not affect the dimensionality reduction process. Note that we considered $\mathbf{x}_{t+1} - \mathbf{x}_t$ to be the output of the C-GPDM dynamic map, [11] suggested that this choice can help to improve the smoothness of latent trajectories. In the following, we report how to model (3) and (4) by means of GPs.

A. Latent variable mapping

Each component of the observation vector $\mathbf{y}_t = [y_t^{(1)}, \dots, y_t^{(D)}]^T$ can be modeled a priori as a zero-mean GP that takes as input \mathbf{x}_t , for $t = 1, \dots, N$.

Let $Y = [\mathbf{y}_1, \dots, \mathbf{y}_N]^T \in \mathbb{R}^{N \times D}$ be the matrix that collects the set of N observations, and $X = [\mathbf{x}_1, \dots, \mathbf{x}_N]^T \in \mathbb{R}^{N \times d}$ be the matrix of associated latent states. We denote with $Y_{:,j}$ the vector containing the j -th components of all the N observations, for $j = 1, \dots, D$.

Then, we have $Y_{:,j} \sim \mathcal{N}(0, K_y^{(j)}(X))$ for $j = 1, \dots, D$. The covariance matrix $K_y^{(j)}(X)$ is defined through a kernel function $k_y^{(j)}(\cdot, \cdot)$. Specifically, for any two observations $r, s = 1, \dots, N$, the covariance between their j -th components $y_r^{(j)}$ and $y_s^{(j)}$, i.e. the element of $K_y^{(j)}(X)$ at row r and column s , is equal to $k_y^{(j)}(\mathbf{x}_r, \mathbf{x}_s)$. The probability distribution of $Y_{:,j}$ is given by

$$p(Y_{:,j}|X) = \frac{\exp\left(-\frac{1}{2}Y_{:,j}^T \left(K_y^{(j)}(X)\right)^{-1} Y_{:,j}\right)}{\sqrt{(2\pi)^N |K_y^{(j)}(X)|}}.$$

If we assume that the D observation components are independent variables, the probability over the whole set of observations can be expressed by the product of the D GPs. In addition, if we choose identical kernel functions for each dimension, with the only difference given by a scaling factor, i.e. $k_y^{(j)}(\cdot, \cdot) = w_{y,j}^{-2} k_y(\cdot, \cdot)$ for $j = 1, \dots, D$, the joint likelihood over the whole set of observations is given by

$$p(Y|X) = \frac{|W_y|^N \exp\left(-\frac{1}{2}\text{tr}\left(\left(K_y^{(j)}(X)\right)^{-1} Y W_y^2 Y^T\right)\right)}{\sqrt{(2\pi)^{ND} |K_y(X)|^D}}, \quad (5)$$

where $W_y = \text{diag}(w_{y,1}, \dots, w_{y,D})$, $K_y(X)$ is the covariance matrix built employing only $k_y(\cdot, \cdot)$, i.e. the common part of kernel functions.

In previous works on GPDMs [10], [11], [12], the GPs of the latent map are usually equipped with a simple form of RBF kernel:

$$k'_y(\mathbf{x}_r, \mathbf{x}_s) = \exp\left(-\frac{\beta_1}{2}\|\mathbf{x}_r - \mathbf{x}_s\|^2\right) + \beta_2^{-1}\delta(\mathbf{x}_r, \mathbf{x}_s), \quad (6)$$

parameterized only by β_1 and β_2 , where $\delta(\mathbf{x}_r, \mathbf{x}_s)$ indicates the Kronecker delta.

Instead, we propose a richer structure for this kernel, characterized by the presence of length-scales that can weight differently each component of the latent state:

$$k_y(\mathbf{x}_r, \mathbf{x}_s) = \exp\left(-\|\mathbf{x}_r - \mathbf{x}_s\|_{\Lambda_y^{-1}}\right) + \sigma_y^2 \delta(\mathbf{x}_r, \mathbf{x}_s). \quad (7)$$

$\Lambda_y^{-1} = \text{diag}(\lambda_{y,1}^{-2}, \dots, \lambda_{y,D}^{-2})$ is a positive definite diagonal matrix, which weights the norm used in the RBF function, and σ_y^2 is the variance of the isotropic noise in (3). The trainable hyper-parameters of the latent map model are then $\theta_y = \{w_{y,1}, \dots, w_{y,D}, \lambda_{y,1}, \dots, \lambda_{y,D}, \sigma_y\}$.

B. Dynamics mapping

Similarly to Sec. III-A, we can model a priori each component of the latent state difference $\mathbf{x}_{t+1} - \mathbf{x}_t = [x_{t+1}^{(1)} - x_t^{(1)}, \dots, x_{t+1}^{(d)} - x_t^{(d)}]^T$ as a zero-mean GP that takes as input the pair $(\mathbf{x}_t, \mathbf{u}_t)$, for $t = 1, \dots, N-1$.

Let $X = [\mathbf{x}_1, \dots, \mathbf{x}_N]^T \in \mathbb{R}^{N \times d}$ be the matrix collecting the set of N latent states, we can denote by $X_{r:s,i}$ the vector of the i -th components from time step r to time step s , with $r, s = 1, \dots, N$. We indicate the vector of differences between consecutive latent states along their i -th component with $\Delta_{:,i} = (X_{2:N,i} - X_{1:N-1,i}) \in \mathbb{R}^{N-1}$. $\Delta = [\Delta_{:,1}, \dots, \Delta_{:,d}] \in \mathbb{R}^{(N-1) \times d}$ is the matrix that collects differences along all the components. Finally, we compactly represent the GP input of the dynamic model as

$$\tilde{\mathbf{x}}_t = \begin{bmatrix} \mathbf{x}_t \\ \mathbf{u}_t \end{bmatrix} \in \mathbb{R}^{d+E},$$

and refer to the the matrix collecting $\tilde{\mathbf{x}}_t$ for $t = 1, \dots, N-1$ with $\tilde{X} = [\tilde{\mathbf{x}}_1, \dots, \tilde{\mathbf{x}}_{N-1}]^T \in \mathbb{R}^{(N-1) \times (d+E)}$.

Thus, we have $\Delta_{:,i} \sim \mathcal{N}(0, K_x^{(i)}(\tilde{X}))$ for $i = 1, \dots, d$. The covariance matrix $K_x^{(i)}(\tilde{X})$ is defined through a kernel function $k_x^{(i)}(\cdot, \cdot)$. Specifically, for any $r, s = 1, \dots, N-1$, the covariance between $x_{r+1}^{(i)} - x_r^{(i)}$ and $x_{s+1}^{(i)} - x_s^{(i)}$, i.e. the element of $K_x^{(i)}(\tilde{X})$ at row r and column s , is equal to $k_x^{(i)}(\tilde{\mathbf{x}}_r, \tilde{\mathbf{x}}_s)$. The probability density over $\Delta_{:,i}$ is then given by

$$p(\Delta_{:,i}|\tilde{X}) = \frac{\exp\left(-\frac{1}{2}\Delta_{:,i}^T \left(K_x^{(i)}(\tilde{X})\right)^{-1} \Delta_{:,i}\right)}{\sqrt{(2\pi)^N |K_x^{(i)}(\tilde{X})|}}.$$

Assuming that the d latent state components evolve independently, the probability over the whole Δ can be expressed by the product of the d GPs. Again, if we choose identical kernel functions for each dimension, with different scaling factors, i.e. $k_x^{(i)}(\cdot, \cdot) = w_{x,i}^{-2} k_x(\cdot, \cdot)$ for $i = 1, \dots, d$, we obtain the following expression for the joint likelihood:

$$p(\Delta|\tilde{X}) = \frac{|W_x|^{N-1} \exp\left(-\frac{1}{2}\text{tr}\left(\left(K_x(\tilde{X})\right)^{-1} \Delta W_x^2 \Delta^T\right)\right)}{\sqrt{(2\pi)^{(N-1)d} |K_x(\tilde{X})|^d}}, \quad (8)$$

where $W_x = \text{diag}(w_{x,1}, \dots, w_{x,d})$, $K_x(\tilde{X})$ is the covariance matrix built employing only $k_x(\cdot, \cdot)$, i.e. the common part of kernel functions.

In standard GPDM [10], dynamic mapping GPs were initially proposed with constant scaling factors $w_{x,i} = 1$ for

$i = 1, \dots, d$, and equipped with a simple "RBF + linear" kernel, characterized only by four trainable parameters:

$$k'_x(\tilde{\mathbf{x}}_r, \tilde{\mathbf{x}}_s) = \alpha_1 \exp\left(-\frac{\alpha_2}{2} \|\tilde{\mathbf{x}}_r - \tilde{\mathbf{x}}_s\|^2\right) + \dots \quad (9)$$

$$\dots + \alpha_3 \tilde{\mathbf{x}}_r^T \tilde{\mathbf{x}}_s + \alpha_4^{-1} \delta(\tilde{\mathbf{x}}_r, \tilde{\mathbf{x}}_s).$$

Analogously to what was previously proposed for the latent mapping, we adopted a more complex kernel function, detailed in the following,

$$k_x(\tilde{\mathbf{x}}_r, \tilde{\mathbf{x}}_s) = \exp\left(-\|\tilde{\mathbf{x}}_r - \tilde{\mathbf{x}}_s\|_{\Lambda_x^{-1}}\right) + \dots \quad (10)$$

$$\dots + [\tilde{\mathbf{x}}_r^T, 1] \Phi [\tilde{\mathbf{x}}_s^T, 1]^T + \sigma_x^2 \delta(\tilde{\mathbf{x}}_r, \tilde{\mathbf{x}}_s).$$

$\Lambda_x^{-1} = \text{diag}(\lambda_{x,1}^{-2}, \dots, \lambda_{x,d+E}^{-2})$ is a positive definite diagonal matrix, which weights the norm used in the RBF component of the kernel. Also $\Phi = \text{diag}(\phi_1^2, \dots, \phi_{d+E+1}^2)$ is a positive definite diagonal matrix that describes the linear component. σ_x^2 is the variance of the isotropic noise in (4). In comparison to (9), the adopted kernel weights differently the various components of the input in both RBF and linear part, where the GP input is also extended as $[\tilde{\mathbf{x}}_s^T, 1]^T$. The trainable hyper-parameters of the dynamic map model are then $\theta_x = \{w_{x,1}, \dots, w_{x,d}, \lambda_{x,1}, \dots, \lambda_{x,d}, \phi_1, \dots, \phi_{d+E+1}, \sigma_x\}$.

Although the parameterization of RBF and linear kernels done in (7) and (10) is a very common practice in GP regression literature [15], to the best of our knowledge it has not been tested before in the context of GPDM.

C. Multiple sequences

It is possible to easily extend the C-GPDM formulation to P multiple sequences of observations, $Y^{(1)}, \dots, Y^{(P)}$, and control inputs, $U^{(1)}, \dots, U^{(P)}$. Let the length of each sequence p , for $p = 1, \dots, P$, be equal to N_p , with $\sum_{p=1}^P N_p = N$. Define the latent states associated to each sequence as $\tilde{X}^{(1)}, \dots, \tilde{X}^{(P)}$. Following the notation of Sec. III-B, define $\tilde{X}^{(1)}, \dots, \tilde{X}^{(P)}$, as the sequence of the aggregated matrices of latent states and control inputs, and $\Delta^{(1)}, \dots, \Delta^{(P)}$ as the difference matrices.

Hence, model joint likelihoods can be calculated by using the following concatenated matrices inside (5) and (8): $Y = [Y^{(1)T} | \dots | Y^{(P)T}]^T$, $X = [X^{(1)T} | \dots | X^{(P)T}]^T$, $\Delta = [\Delta^{(1)} | \dots | \Delta^{(P)}]^T$ and $\tilde{X} = [\tilde{X}^{(1)T} | \dots | \tilde{X}^{(P)T}]^T$. Note that, when dealing with multiple sequences, the number of data points in the dynamic mapping becomes $N - P$, and expression (8) must be adapted accordingly.

IV. C-GPDM TRAINING AND PREDICTIONS

Training the C-GPDM entails using numerical optimization techniques to estimate the unknowns in the model, i.e., latent states X and the hyper-parameters θ_x, θ_y . Latent coordinates X are initialized by means of PCA [17], selecting the first d principal components of Y . A natural approach for training C-GPDMs is to minimize the joint negative log-likelihood $-\ln p(Y|X) = -\ln p(Y|X) - \ln p(\Delta|\tilde{X})$ w.r.t. $\{X, \theta_x, \theta_y\}$. As regards numerical optimization, we used the L-BFGS algorithm [18] implemented with PyTorch [19].

Hence, the overall loss will be given, up to an additive constant, by

$$\mathcal{L} = \mathcal{L}_y + \mathcal{L}_x, \quad (11)$$

where

$$\mathcal{L}_y = \frac{D}{2} \ln |K_y(X)| + \frac{1}{2} \text{tr}(K_y(X)^{-1} Y W_y^2 Y^T) - N \ln |W_y|,$$

$$\mathcal{L}_x = \frac{d}{2} \ln |K_x(\tilde{X})| + \frac{1}{2} \text{tr}(K_x(\tilde{X})^{-1} \Delta W_x^2 \Delta^T) - (N-1) \ln |W_x|.$$

In case the C-GPDM is trained on multiple sequences of inputs and observations, make sure to employ the aggregated matrices defined in Sec. III-C when computing loss function 11. It is also necessary to use the factor $N - P$ instead of $N - 1$ inside the expression of \mathcal{L}_x .

A trained C-GPDM can be used to fulfill two different purposes: (i) map a given new latent state \mathbf{x}_t^* to the corresponding \mathbf{y}_t^* in observation space, (ii) predict the evolution of the latent state at the next time step \mathbf{x}_{t+1}^* , given \mathbf{x}_t^* and a certain control action \mathbf{u}_t^* . The two processes, together, can be used to predict the sequence of observations produced by applying a series of control actions to the system.

A. Latent prediction

Given \mathbf{x}_t^* , the probability density of its corresponding observation \mathbf{y}_t^* is $p(\mathbf{y}_t^* | \mathbf{x}_t^*, X, \theta_y) = \mathcal{N}(\mu_y(\mathbf{x}_t^*), v_y(\mathbf{x}_t^*) W_y^{-2})$, with

$$\mu_y(\mathbf{x}_t^*) = Y^T K_y(X)^{-1} \mathbf{k}_y(\mathbf{x}_t^*, X)$$

$$v_y(\mathbf{x}_t^*) = k_y(\mathbf{x}_t^*, \mathbf{x}_t^*) - \mathbf{k}_y(\mathbf{x}_t^*, X)^T K_y(X)^{-1} \mathbf{k}_y(\mathbf{x}_t^*, X),$$

where $\mathbf{k}_y(\mathbf{x}_t^*, X) = [k_y(\mathbf{x}_t^*, \mathbf{x}_1), \dots, k_y(\mathbf{x}_t^*, \mathbf{x}_N)]^T$.

B. Dynamics prediction

Given \mathbf{x}_t^* and \mathbf{u}_t^* , let's define $\tilde{\mathbf{x}}_t^* = [\mathbf{x}_t^{*T}, \mathbf{u}_t^{*T}]^T$. The probability density of the latent state at the next time step \mathbf{x}_{t+1}^* is $p(\mathbf{x}_{t+1}^* | \tilde{\mathbf{x}}_t^*, X, \theta_x) = \mathcal{N}(\mu_x(\mathbf{x}_t^*), v_x(\mathbf{x}_t^*) W_x^{-2})$, with

$$\mu_x(\mathbf{x}_t^*) = \mathbf{x}_t^* + \Delta^T K_x(\tilde{X})^{-1} \mathbf{k}_x(\tilde{\mathbf{x}}_t^*, \tilde{X}),$$

$$v_x(\mathbf{x}_t^*) = k_x(\tilde{\mathbf{x}}_t^*, \tilde{\mathbf{x}}_t^*) - \mathbf{k}_x(\tilde{\mathbf{x}}_t^*, \tilde{X})^T K_x(\tilde{X})^{-1} \mathbf{k}_x(\tilde{\mathbf{x}}_t^*, \tilde{X}),$$

where $\mathbf{k}_x(\tilde{\mathbf{x}}_t^*, \tilde{X}) = [k_x(\tilde{\mathbf{x}}_t^*, \tilde{\mathbf{x}}_1), \dots, k_x(\tilde{\mathbf{x}}_t^*, \tilde{\mathbf{x}}_{N-1})]^T$.

C. Trajectory prediction

Starting from an initial latent state \mathbf{x}_1^* , one can predict the evolution of the system over a desired horizon of length N_d , when subject to a given sequence of control actions $\mathbf{u}_1^*, \dots, \mathbf{u}_{N_d-1}^*$. At each time step $t = 1, \dots, N_d - 1$, \mathbf{x}_{t+1}^* can be sampled from the normal distribution $p(\mathbf{x}_{t+1}^* | \tilde{\mathbf{x}}_t^*, X, \theta_x)$ defined in Sec. IV-B. Hence, the generated trajectory in the latent space $\mathbf{x}_1^*, \dots, \mathbf{x}_{N_d}^*$ can be mapped into the associated predicted sequences of observations $\mathbf{y}_1^*, \dots, \mathbf{y}_{N_d}^*$ by mean of $p(\mathbf{y}_t^* | \mathbf{x}_t^*, X, \theta_y)$, defined in Sec. IV-A.

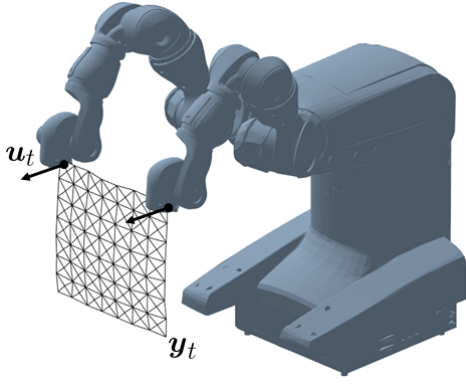


Fig. 2: Simulated setup for cloth manipulation with bimanual robot. The cloth is positioned in its starting configuration. Observations \mathbf{y}_t are the positions of the points in the mesh representing the cloth. Control actions \mathbf{u}_t are the differences between consecutive commanded end-effectors' positions.

V. EXPERIMENT: MODELING CLOTH MANIPULATION

As regards to the experimental application, we considered a simulated scenario, consisting of a bimanual robot that moves a piece of cloth by holding its two upper corners. The cloth is modeled as an 8×8 mesh of material points. The two points in the upper corners are assumed to be attached to the two robot's end-effectors, while the other points move following the dynamical model proposed in [20]. In this context, the observation vector is given by the Cartesian coordinates of all the points in the mesh; hence $\mathbf{y}_t \in \mathbb{R}^D$ with $D = 192$ (measured in meters). We assume that the two end-effectors can be controlled exactly in the operational space. In this system, the controls acting at time step t are the differences between position commands at instant $t + 1$ and t ; so $\mathbf{u}_t \in \mathbb{R}^E$ with $E = 6$ (measured in meters). The overall setup is shown in Fig. 2. The objective of the experiment is to learn the high-dimensional cloth dynamics using C-GPDM, in order to make predictions about cloth movements in response to sequences of control actions that were not seen during training. Specifically, we would like to evaluate how much the prediction accuracy is affected by

- the number of observation sequences used for training,
- the range of the considered cloth movements,
- the choice of the kernel functions.

We adopted a latent space of dimension $d = 3$, resulting in a dimensionality reduction factor of $D/d = 64$.

A. Data collection

Data were obtained by recording observation trajectories associated to several types of cloth oscillation, obtained by applying different sequences of control actions. All the considered trajectories start from the same cloth configuration and last 5 seconds. Observations were recorded each 0.05 seconds, hence $N = 100$ total number of steps for each sequence.

Let $\mathbf{u}_t = [r \delta_t^X, r \delta_t^Y, r \delta_t^Z, l \delta_t^X, l \delta_t^Y, l \delta_t^Z]^T$, where $r \delta_t^X, r \delta_t^Y$ and $r \delta_t^Z$ ($l \delta_t^X, l \delta_t^Y$ and $l \delta_t^Z$) indicate the displacement of the

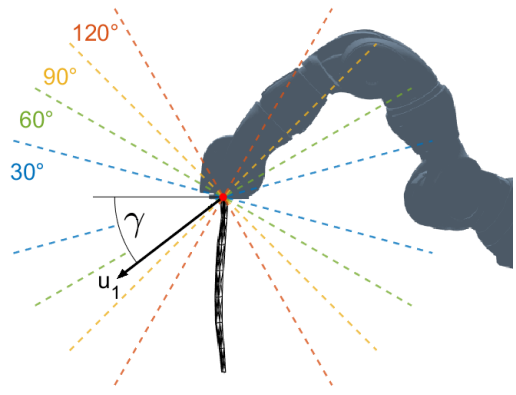


Fig. 3: Representation of the movement ranges within which control parameter γ was sampled during data collection.

right (left) end-effector position along the three Cartesian axes, between step t and $t + 1$. Thus, the applied \mathbf{u}_t were such that,

$$r \delta_t^X = 0 \quad (12a)$$

$$r \delta_t^Y = -0.01 \cos(\gamma) \cos(2\pi f_Y t) \quad (12b)$$

$$r \delta_t^Z = 0.01 \sin(\gamma) \cos(2\pi f_Z t) \quad (12c)$$

$$l \delta_t^X = 0 \quad (12d)$$

$$l \delta_t^Y = -0.01 \cos(\gamma) \cos(2\pi f_Y t) \quad (12e)$$

$$l \delta_t^Z = 0.01 \sin(\gamma) \cos(2\pi f_Z t). \quad (12f)$$

Such controls make the robot's end-effectors oscillate on the Y-Z plane of the operational space. Parameter γ can be interpreted as the inclination of \mathbf{u}_1 w.r.t. the horizontal, and it loosely defines a direction of the oscillation. On the other hand, f_Y and f_Z define the frequencies of the oscillations along the axes. If they are similar, the end-effectors move mostly along the direction defined by γ , if not, the oscillation takes place in a broader space.

In order to obtain an heterogeneous set of trajectories for the composition of training and test sets, we collected several movements obtained by choosing in a random fashion the control parameters γ, f_Y and f_Z . Angles γ could be uniformly sampled inside a variable range $[-\frac{R}{2}, \frac{R}{2}]$ (deg), we indicate the movement range with the amplitude of its angular area, R (deg). Instead, frequencies f_Y and f_Z were uniformly sampled inside the fixed interval $[0.3, 0.6]$ (Hz).

We considered four movement ranges of increasing size, namely $R \in \{30, 60, 90, 120\}$ (see Fig. 3), and collected a specific data-set \mathcal{D}_R associated to each range. Every set contains 50 cloth trajectories obtained by applying control actions of the form (12) with 50 different random choices for parameters γ, f_Y and f_Z . From each collection \mathcal{D}_R , 10 trajectories were extracted and used as test sets \mathcal{D}_R^{test} for the corresponding movement range, while training sets \mathcal{D}_R^{train} were built with the remaining sequences.

B. Training models

The objective of the experiment is to evaluate C-GPDM prediction accuracy in different movement ranges, and for

different amounts of training data. Also, we want to observe if the proposed kernel functions, (7) and (10), are beneficial, in terms of prediction accuracy, w.r.t. standard GPDM kernel functions, (6) and (9).

Consequently, for each considered movement range R , we trained different C-GPDMs, equipped with the proposed kernels, employing an increasing number of sequences randomly picked from \mathcal{D}_R^{train} . Specifically, we used 10 different combinations of 5, 10, 15 and 20 sequences for each range. In this way, we were able to reduce the dependencies on the specific training trajectories employed, and to average prediction accuracy over different possible sets of training data. For each such model, a C-GPDM equipped with standard kernels was trained on exactly the same data.

C. Results

We used each learned C-GPDM to predict the cloth movements when subject to the test control actions relative to the related \mathcal{D}_R^{test} , for $R \in \{30, 60, 90, 120\}$. Let $\mathbf{y}_t^{(R,k)}$ and $\mathbf{u}_t^{(R,k)}$ denote the observation and control actions, at time step t , of the k -th test trajectory in \mathcal{D}_R^{test} .

For every considered range R , one can follow the procedure described in Sec. IV-C and employ the trained C-GPDMs to predict the trajectories resulting from the application of control action sequences $\{\mathbf{u}_t^{(R,k)}\}_{t=1}^{N-1}$, for $k = 1, \dots, 10$. Let $\mathbf{x}_t^{*(R,k)}$ be the predicted latent state at time t , and $\mathbf{y}_t^{*(R,k)}$ the corresponding predicted observation. There is a degree of freedom in the choice of the initial latent state. Since in the GPDM formulation, an explicit map from observation to latent space is not given; there is no principled way to choose $\mathbf{x}_1^{*(R,k)}$ given an unseen $\mathbf{y}_1^{*(R,k)}$. But, in the context of this experiment, all the cloth movements adopted for training and test started from the same configuration. Hence, we could select $\mathbf{x}_1^{*(R,k)}$ equal to the latent state associated to the first observation of the training trajectories.

By visualization of the predicted movements, we can state that C-GPDMs, trained with a sufficient amount of data (10, 15 and 20 sequences in this example), are able to capture the cloth dynamics of oscillations along axes Y and Z. Such models obtained satisfying results in a variety of movement ranges. In fact, for smaller movement ranges ($R = 30$ or $R = 60$), the reconstructed trajectories of the mesh of points appear very similar to the true ones. On the other hand, for wider ranges ($R = 90$ or $R = 120$), discrepancies between true and predicted points begin to be more evident, but the C-GPDMs are still able to predict the overall movement of the piece of cloth quite nicely. In Fig. 5 we report a series of video frames showing the original cloth movement and the relative prediction. Please look at the video included in the auxiliary materials to better appreciate the result.

In order to measure the prediction accuracy of the obtained results, we define the following error function:

$$\epsilon^{(R,k)} = 100 \cdot \sum_{t=1}^N \frac{\|\mathbf{y}_t^{(R,k)} - \mathbf{y}_t^{*(R,k)}\|}{\|\mathbf{y}_t^{(R,k)}\|}, \quad (13)$$

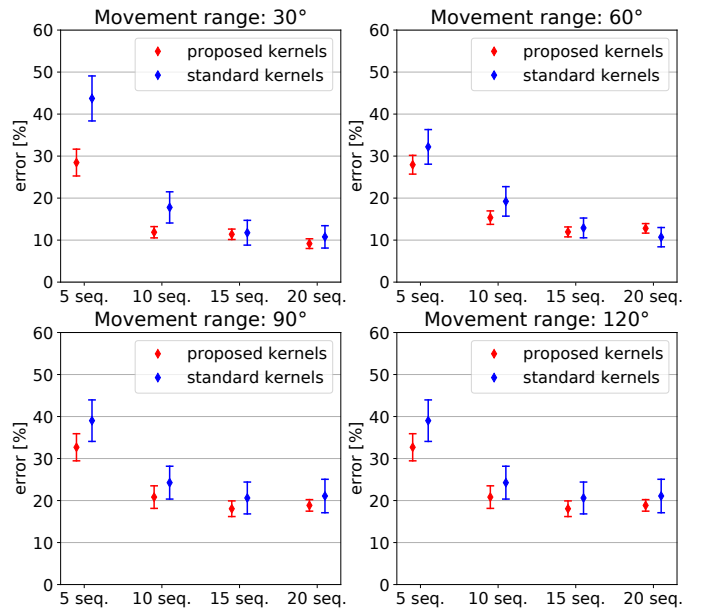


Fig. 4: Mean relative errors (with 95% C.I.) obtained by different C-GPDM setups in the considered movement ranges. Results obtained by the proposed kernels, (7) and (10), are indicated in red, those obtained with the standard kernels, (6) and (9), in blue.

that expresses the cumulative prediction error w.r.t. a certain test trajectory, as a percentage of the cumulative magnitude of the true sequence of observations.

In Fig. 4, we report, for all the movement ranges, the errors (13) obtained in the test sets by different C-GPDMs averaging the results over random training set composition. Results are indicated with mean and 95% confidence interval.

As it was natural to expect, C-GPDMs trained with only 5 sequences show higher errors than the models trained employing more data. But the resulting errors do not always diminish with the increase in the amount of training trajectories. In fact, in all the considered movement ranges, accuracy does not considerably change passing from 15 training sequences to 20. Moreover, the proposed kernels seem able to slightly improve accuracy and consistency of the results in the majority of cases. This effect is clearer in a low-data regime, with models trained on 5 or 10 sequences.

VI. CONCLUSIONS

We presented an extension of the GPDM framework able to incorporate control actions in its definition, we call it *Controlled Gaussian Process Dynamical Model* (C-GPDM). Such framework is intended to model complex high-dimensional dynamics governed by control actions, by projecting observation space into a latent space of lower dimensionality, where dynamical relations are easier to infer. Alongside, we proposed alternative kernel functions for both latent mapping and dynamics, characterized by a richer parameterization than the standard one adopted in most previous GPDM realizations.

C-GPDMs were tested in a simulated scenario of robotic cloth manipulation. Specifically, we considered a bimanual

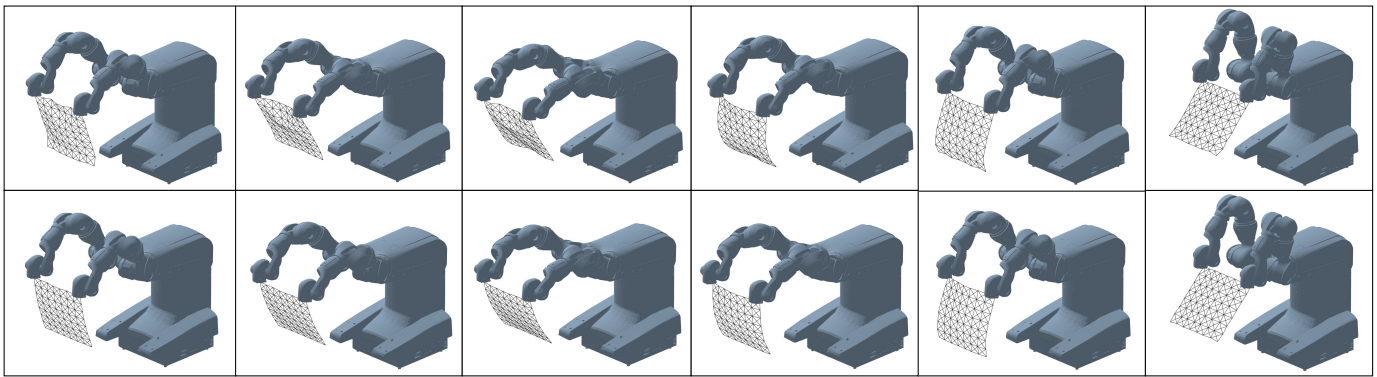


Fig. 5: (Top) Frames recorded from a simulated cloth movement. (Bottom) Corresponding predictions obtained by C-GPDM.

robot moving a piece of cloth by holding it from its two upper corners. The cloth was represented as an 8×8 mesh of points, resulting in an observation vector that comprises all their Cartesian coordinates, for a total dimension of $D = 192$. Several realizations of C-GPDM were trained and tested on a sufficiently varied data-set of trajectories to project the cloth movement into a latent space of dimension $d = 3$. The presented model was able to learn the complex high-dimensional dynamics of the cloth oscillations determined by the end-effectors movement. Furthermore, the adopted kernel functions proved to be beneficial in terms of prediction accuracy.

Future work involves the application of C-GPDM to data collected on a real cloth manipulation experiment, where the movements are registered by means of camera images, trackers, depth sensors, etc. Such scenario is characterized by many challenges, like the presence of measurement noise and missing data. C-GPDMs may also be employed in a model-based reinforcement learning framework that relies on GPs, such as [21], [22], to handle the modeling of high-dimensional dynamics, that could be unfeasible to approach without applying dimensionality-reduction techniques. Finally, the proposed C-GPDM formulation could be extended through the introduction of back constraints [23] to preserve local distances and obtain an explicit formulation of the mapping from the observation to latent space.

REFERENCES

- [1] D. Terzopoulos, J. Platt, A. Barr, and K. Fleischer, "Elastically deformable models," *SIGGRAPH Comput. Graph.*, vol. 21, no. 4, pp. 205–214, 1987.
- [2] D. Baraff and A. Witkin, "Large steps in cloth simulation," *Association for Computing Machinery*, pp. 43–54, 1998.
- [3] A. Nealen, M. Müller, R. Keiser, E. Boxerman, and M. Carlson, "Physically based deformable models in computer graphics," *Computer Graphics Forum*, vol. 25, pp. 809–836, 2006.
- [4] D. Baraff and A. Witkin, "Dexterous manipulation of cloth," *Computer Graphics Forum*, vol. 35, no. 2, pp. 523–532, 2016.
- [5] A. Colomé and C. Torras, "Dimensionality reduction for dynamic movement primitives and application to bimanual manipulation of clothes," *IEEE Transactions on Robotics*, vol. 34, no. 3, pp. 602–615, 2018.
- [6] N. Lawrence and A. Hyvärinen, "Probabilistic non-linear principal component analysis with gaussian process latent variable models," *Journal of machine learning research*, vol. 6, no. 11, 2005.
- [7] N. Koganti, T. Shibata, T. Tamei, and K. Ikeda, "Data-efficient learning of robotic clothing assistance using bayesian gaussian process latent variable model," *Advanced Robotics*, vol. 33, pp. 1–15, 04 2019.
- [8] J. A. Delgado-Guerrero, A. Colomé, and C. Torras, "Contextual policy search for micro-data robot motion learning through covariate gaussian process latent variable models," in *2020 IEEE/RSJ International Conference on Intelligent Robots and Systems*, 2020, pp. 5511–5517.
- [9] N. Koganti, T. Tamei, K. Ikeda, and T. Shibata, "Bayesian nonparametric learning of cloth models for real-time state estimation," *IEEE Transactions on Robotics*, vol. 33, no. 4, pp. 916–931, 2017.
- [10] J. M. Wang, A. Hertzmann, and D. J. Fleet, "Gaussian process dynamical models," *Advances in neural information processing systems*, vol. 18, pp. 1441–1448, 2005.
- [11] J. M. Wang, D. J. Fleet, and A. Hertzmann, "Gaussian process dynamical models for human motion," *IEEE transactions on pattern analysis and machine intelligence*, vol. 30, no. 2, pp. 283–298, 2007.
- [12] R. Urtasun, D. J. Fleet, and P. Fua, "3d people tracking with gaussian process dynamical models," in *2006 IEEE Computer Society Conference on Computer Vision and Pattern Recognition (CVPR'06)*, vol. 1. IEEE, 2006, pp. 238–245.
- [13] Z. Zhu, X. You, S. Yu, J. Zou, and H. Zhao, "Dynamic texture modeling and synthesis using multi-kernel gaussian process dynamic model," *Signal Processing*, vol. 124, pp. 63–71, 2016.
- [14] N. Koganti, J. G. Ngeo, T. Tomoya, K. Ikeda, and T. Shibata, "Cloth dynamics modeling in latent spaces and its application to robotic clothing assistance," in *2015 IEEE/RSJ International Conference on Intelligent Robots and Systems (IROS)*. IEEE, 2015, pp. 3464–3469.
- [15] C. E. Rasmussen, "Gaussian processes in machine learning," in *Summer School on Machine Learning*. Springer, 2003, pp. 63–71.
- [16] P. Li and S. Chen, "A review on gaussian process latent variable models," in *CAAI Transactions on Intelligence Technology*, vol. 1, 2016, pp. 366–376.
- [17] C. M. Bishop, *Pattern recognition and machine learning*. Springer, 2006.
- [18] R. H. Byrd, P. Lu, J. Nocedal, and C. Zhu, "A limited memory algorithm for bound constrained optimization," *SIAM Journal on scientific computing*, vol. 16, no. 5, pp. 1190–1208, 1995.
- [19] A. Paszke, S. Gross, F. Massa, A. Lerer, J. Bradbury, G. Chanan, T. Killeen, Z. Lin, N. Gimelshein, L. Antiga, A. Desmaison, A. Kopf, E. Yang, Z. DeVito, M. Raison, A. Tejani, S. Chilamkurthy, B. Steiner, L. Fang, J. Bai, and S. Chintala, "Pytorch: An imperative style, high-performance deep learning library," in *Advances in Neural Information Processing Systems* 32, 2019, pp. 8024–8035.
- [20] F. Coltraro Ianniello, "Experimental validation of an inextensible cloth model," *Technical Report IRI-TR-20-04, Institut de Robòtica i Informàtica Industrial, CSIC-UPC, UPCommons*, 2020.
- [21] K. Chatzilygeroudis, R. Rama, R. Kaushik, D. Goepf, V. Vassiliades, and J.-B. Mouret, "Black-box data-efficient policy search for robotics," in *2017 IEEE/RSJ International Conference on Intelligent Robots and Systems (IROS)*. IEEE, 2017, pp. 51–58.
- [22] F. Amadio, A. D. Libera, R. Antonello, D. Nikovski, R. Carli, and D. Romeres, "Model-based policy search using monte carlo gradient estimation with real systems application," *arXiv preprint:2101.12115*, 2021.
- [23] N. D. Lawrence and J. Quinero-Candela, "Local distance preservation in the gp-lvm through back constraints," in *Proceedings of the 23rd international conference on Machine learning*, 2006, pp. 513–520.